SCIENTIFIC REPORTS

OPEN

SUBJECT AREAS:
CONDENSED-MATTER PHYSICS
QUANTUM PHYSICS
THEORY AND COMPUTATION
NANOSCALE MATERIALS

Received
21 August 2013

Accepted
17 January 2014

Published
7 February 2014

Correspondence and requests for materials should be addressed to U.S. (udo.schwingenschlogl@kaust.edu.sa)

Pressure controlled transition into a self-induced topological superconducting surface state

Zhiyong Zhu, Yingchun Cheng & Udo Schwingenschlögl

Physical Sciences and Engineering Division, KAUST, Thuwal 23955-6900, Kingdom of Saudi Arabia.

Ab-initio calculations show a pressure induced trivial-nontrivial-trivial topological phase transition in the normal state of 1*T*-$TiSe_2$. The pressure range in which the nontrivial phase emerges overlaps with that of the superconducting ground state. Thus, topological superconductivity can be induced in protected surface states by the proximity effect of superconducting bulk states. This kind of self-induced topological surface superconductivity is promising for a realization of Majorana fermions due to the absence of lattice and chemical potential mismatches. For appropriate electron doping, the formation of the topological superconducting surface state in 1*T*-$TiSe_2$ becomes accessible to experiments as it can be controlled by pressure.

Majorana fermions are half integer spin particles that are their own antiparticles[1]. In a two-dimensional superconductor, a vortex with an odd number of Majorana quasiparticle excitations obeys non-Abelian rather than the Bose or Fermi statistics[2–4]. The states are robust against local noise and, hence, are considered as strong candidates for a fault tolerant quantum information processing[4]. Initially, Majorana quasiparticle excitations have been predicted to occur in topological superconducting phases in which the Cooper pairs have a spin-triplet $p_x + ip_y$ pairing symmetry[5]. This case is very rare in nature. The most promising system is the exotic p-wave superconductor Sr_2RuO_4[6,7] for which the experimental situation, however, is not clear[8,9].

Later, they also have been proposed to appear in topological superconducting interface states. This would enable induction by the conventional s-wave superconducting proximity effect on the Dirac-like boundary states of topological insulators[10,11], of half-metallic materials[12,13], and of semiconductors with substantial Rashba spin-orbit coupling[14,15]. Recently, superconductivity has been reported for the prototypical three-dimensional topological insulators Bi_2Se_3 and Bi_2Te_3[16–19] under doping[20–24] and under pressure[25]. Accordingly, topological superconductivity is predicted to be induced by the superconducting proximity effect on topologically protected Dirac-like surface states of the superconductor itself[20,22]. Such a self-induced topological surface superconductor is very promissing for the realization of Majorana quasiparticle exitations due to the absence of lattice and chemical potential mismatches[21].

1*T*-$TiSe_2$ is one of the early discovered materials with a charge density wave (CDW)[26], and has seen a revival of interest due to recently discovered superconductivity[27–35]. It is a layered compound, consisting of slabs in which Ti is octahedrally coordinated by six Se atoms. Se-Ti-Se slabs with ionic bonding are separated by a van der Waals gap, leading to a quasi two-dimensional nature. A commensurate CDW with a $2 \times 2 \times 2$ superstructure developes below 200 K[26]. No sign of superconductivity is found by lowering the temperature only. However, under controlled Cu-intercalation into the van der Waals gap the CDW is progressively suppressed and a superconducting state emerges with a maximum transition temperature of $T_c = 4.15$ K[27]. Suppression of the CDW and emergence of superconductivity have been discovered in pressurized 1*T*-$TiSe_2$ with a maximum T_c of 1.8 K[34].

In the following, we apply fully-relativistic all-electron ab-initio calculations to reveal a pressure induced trivial-nontrivial-trivial topological phase transition in the normal state of 1*T*-$TiSe_2$. We argue that the pressure range of the topologically nontrivial phase overlaps with that of the superconductivity. Our findings suggest pressurized 1*T*-$TiSe_2$ as another candidate for self-induced topological surface superconductivity for appropriate doping.

Results

Experimental values of the structure parameters have not been determined for pressurized 1*T*-$TiSe_2$ and theoretical calculations encounter serious deficiencies in predicting the parameters for 1*T*-layered compounds under

pressure[36]. Our calculations confirm this observation. The structure parameters of 1*T*-$TiSe_2$ at ambient pressure show errors of −1% (2%), −3% (9%), and 4% (−7%) for the values of *a*, *c*, and *z*, respectively, employing the local density (generalized gradient) approximation. These errors are problematic because of a high sensitivity of the electronic states to the structure, see also the text below. The generalized gradient approximation with explicitly treated van der Waals interaction leads to even worse errors of 5%, 8%, and 5% for the three parameters. On the other hand, the experimental structure is available for 1*T*-TiS_2 under pressure[37]. The similarity of the crystal structure and chemical composition[38] justifies to adopt the values of a/a_0, c/c_0, and *z* of 1*T*-TiS_2 for the normal state of pressurized 1*T*-$TiSe_2$, which we make use of in the following. Note that the crystal symmetry of the high-temperature normal phase is adopted for the entire pressure range, although a CDW transition with lattice distortion appears at low temperature for a pressure below 2 GPa. We will argue that this assumption does not affect the conclusions of our work.

The fully-relativistic electronic band structure of the normal state of 1*T*-$TiSe_2$ at ambient pressure is depicted in Fig. 1(b). The observed energy overlap of the valence band maximum (VBM) and conduction band minimum (CBM) indicates a semimetallic nature. The almost full valence and almost empty conduction bands show mainly Se 4*p* and Ti 3*d* characters, respectively, indicating an overall ionic bonding with charge transfer from Ti to Se. Near E_F the electronic structure of 1*T*-$TiSe_2$ is governed by two bands, giving rise to the hole-like Se 4*p* derived VBM at the Γ-point and the electron-like Ti 3*d* derived CBM at the L-point. The space inversion symmetry of 1*T*-$TiSe_2$ allows us to calculate the band topological invariants by the parity check method proposed by Fu and Kane[39]. Due to the semimetallic nature, however, one needs to consider the valence states instead of the occupied states below E_F. The $\mathbb{Z}_2$ topological invariant can be calculated directly from knowledge about the parity of each pair of Kramers degenerate bands up to the local VBMs at the eight time-reversal momenta (1Γ, 3M, 1A, and 3L). A value of zero is obtained for all four $\mathbb{Z}_2$ topological invariants, reflecting a topologically trivial nature of the normal state of 1*T*-$TiSe_2$ at ambient pressure.

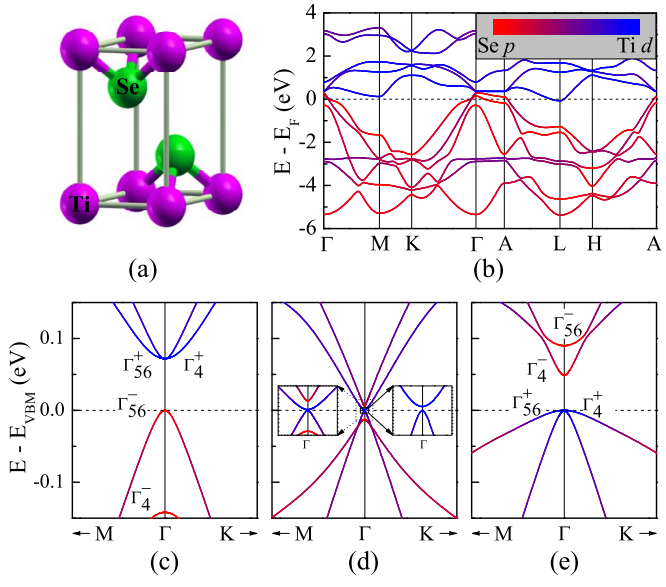

Figure 1 | Normal state of 1*T*-$TiSe_2$. (a) Crystal structure. (b) Electronic band structure at ambient pressure. (c–e) Detailed band structures near the VBM under ambient pressure, 3 GPa, and 5 GPa, respectively. It should be noted that the Fermi energy is located around 0.5 eV below the VBM.

Due to the smaller energy gap around the Γ-point, as compared to the other seven time-reversal momenta, the band topology is mainly defined by the band order at the Γ-point, on which we focus in the following. A zoom of the VBM is displayed in Fig. 1(c) for ambient pressure. Below E_{VBM}, we see two spin-orbit split Se $4p_{x,y}$ states: the lower doublet Γ_4^- and the upper doublet Γ_{56}^-, where the latter forms the VBM. Above E_{VBM}, the spin-orbit coupling lifts the degeneracy of the Ti $3d_{xz,yz}$ states and yields the lower doublet Γ_4^+ and the upper doublet Γ_{56}^+. Under sufficient pressure, the odd parity Se $4p$ Γ_{56}^- state is pushed on top of the Ti $3d$ Γ_4^+ state with even parity. As an example, Fig. 1(d) illustrates the band structure of the normal state of 1*T*-$TiSe_2$ under a pressure of 3 GPa. We find that the band order is not changed at the other seven time-reversal invariant momenta.

According to the parity check method for calculating topological invariants, inversion of bands with a different parity at the Γ-point transforms 1*T*-$TiSe_2$ into a topologically nontrivial state of (1;000) type. The same topological phase transition due to pressure induced band inversion has been observed in layered GaS and GaSe[40]. For higher pressure, the odd parity Se $4p$ Γ_4^- state is pushed above the Ti $3d$ Γ_{56}^+ state with even parity, see the band structure in Fig. 1(e) for a pressure of 5 GPa. As a result, the band topology switches back to trivial. Therefore, we are confronted with a pressure induced trivial-nontrivial-trivial topological phase transition in the normal state of 1*T*-$TiSe_2$.

The phase transition may be viewed as a result of the small energy gap at the VBM and, hence, the sensitivity of the band hierarchy against modifications of the structure. In addition, spin-orbit coupling is crucial for its occurrence and the appearance of a topologically nontrivial phase. Without spin-orbit coupling, the Se $4p_{x,y}$ Γ_4^- and Γ_{56}^- states would form a degenerate pair. Under pressure these odd parity states would simultaneously be pushed above the even parity Ti $3d$ states and no phase transition would be observed. Therefore, an energy difference between the Γ_{56}^- and Γ_4^- states is necessary for the emergence of a pressure induced topological phase transition. In the present case, the energy difference is caused by the spin-orbit coupling. It determines the pressure range of the topologically nontrivial phase. Specifically, the critical pressures of the trivial-nontrivial (p_c') and nontrivial-trivial (p_c'') transitions, are related to the energy differences between Γ_{56}^- and Γ_4^+ (Δ_E') and Γ_4^- and Γ_{56}^+ (Δ_E''), respectively. Accordingly, the topological phase diagram of the normal state of 1*T*-$TiSe_2$ under pressure can be derived from the band order. The result is shown in Fig. 2(a) for pressures between 1.5 and 4.5 GPa.

Figure 2(a) includes the experimental pressure phase diagram for the ground state. We obtain $p_c' = 2.7$ GPa and $p_c'' = 3.2$ GPa. On the other hand, experiments for sub-Kelvin temperature point to pressure induced phase transitions from CDW to superconductor to the normal state[34]. With increasing pressure, the superconductivity appears around 2 GPa and disappears beyond 4 GPa. The pressure range p_c' to p_c'' overlaps with the range in which the superconducting ground state develops. Since the band hierarchy is sensitive to the structure parameters, the pressure range p_c' to p_c'' could depend on uncertainties in the structure determination. Using the data set reported in Ref. 41 for a/a_0, c/c_0, and *z*, we obtain another topological phase diagram, which is depicted in Fig. 2(b). The pressure range p_c' to p_c'' changes substantially with respect to Fig. 2(a), but still overlaps with the range of the superconducting ground state. As mentioned above, a hypothetical crystal symmetry without CDW distortion is used for pressures lower than 2 GPa, which, however, is in the range where our assumption on the crystal symmetry does not influence the conclusions. The discrepancy between the two experimental sets of lattice constants concerns mainly the value of c/c_0. For a pressure of 3 GPa, for example, the difference is 0.1% for a/a_0 but 0.7% for c/c_0. This leads to a 0.1 GPa shift for p_c' and a much larger shift of 1 GPa for p_c''. Therefore, as long as p_c' is in the pressure range from 2 GPa to 4 GPa, the range of the nontrivial phase will overlap with

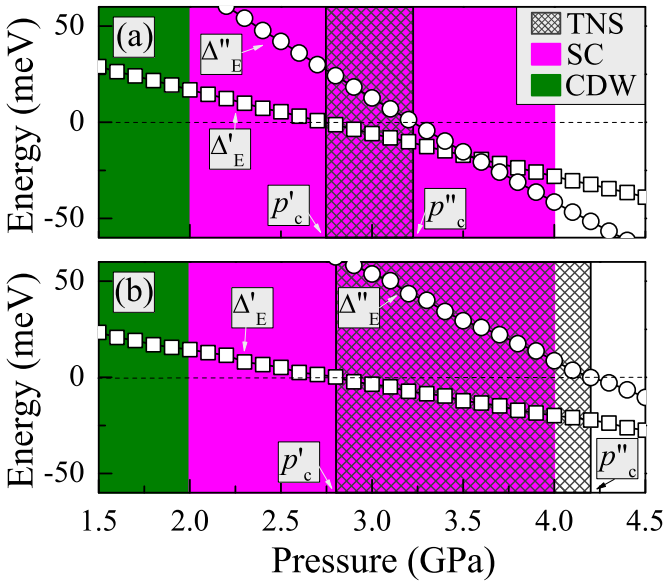

Figure 2 | (a) Topological phase diagram of the normal state of 1*T*-$TiSe_2$ under pressure. Δ'_E and Δ''_E represent the energy differences of the Γ_{56}^- and Γ_4^+ states and of the Γ_4^- and Γ_{56}^+ states, respectively. The experimental pressure phase diagram of the ground state is also sketched. TNS, SC, and CDW denote the topologically nontrivial state, the superconducting ground state, and the charge density wave ground state, respectively. (b) Same as (a) but for another set of a/a_0, c/c_0, and z, see the text for details.

the superconducting ground state. This means that our conclusions stay valid even when the discrepancy in the experimental lattice constant is 10 to 20 times larger than that of Refs. 37 and 41. One of the most important consequences of a topologically nontrivial state is the existence of a gapless surface state[39,42–48], which is protected by the combination of spin-orbit coupling and time-reversal symmetry and shows a spin-textured Dirac-like behavior[16–19,49]. Therefore, our results indicate that a superconducting ground state coexists with a topologically protected spin-textured Dirac-like surface state near the VBM in pressurized 1*T*-$TiSe_2$.

If bulk superconductivity develops in pressurized 1*T*-$TiSe_2$ at low temperature, Cooper pairs can tunnel from the bulk states into the surface states. An *s*-wave pairing symmetry is to be expected, because the bulk superconducting phase is governed by electron-phonon coupling[35]. This leads to the induction of a *s*-type superconducting energy gap in the Dirac-like surface states[10]. Note that the superconducting ground state persists for slight Cu-intercalation in pressurized 1*T*-$TiSe_2$[31,34]. By Cu-intercalation, the tunneling process can be enhanced because E_F is shifted close to the VBM, hence to the Dirac-like surface states. The resulting two-dimensional superconducting surface state resembles the spinless $p_x + ip_y$ topological superconductor, except that the time-reversal symmetry is not violated[10]. Like the $p_x + ip_y$ superconductor, the induced surface superconductor will have a Majorana quasiparticle excitation bound to a vortex[10]. We thus propose pressurized 1*T*-$TiSe_2$ as a material in which topological superconductivity is induced by the superconducting proximity effect on topologically protected spin-textured Dirac-like surface states of the superconductor itself. Such a self-induced surface topological superconductivity is promising as it is free of lattice and chemical potential mismatches. Self-induced topological surface superconductivity before has been predicted for Bi_2Se_3 and Bi_2Te_3 under both doping and pressure[20,22]. The semimetallic nature and formation of a hole pocket at the VBM found in our calculations indicate that the surface Dirac-like states are not located at E_F, making electron doping necessary. Assuming a rigid band model, a doping of 0.7 electrons per formular unit is required to shift E_F by 0.5 eV. A shift of more than 0.1 eV has been demonstrated for a formal doping of 0.065 electrons without losing the superconductivity[30]. Preservation for higher doping calls for experimental confirmation.

Discussion

In conclusion, we have applied density functional theory to demonstrate a pressure induced trivial-nontrivial-trivial topological phase transition for the normal state of 1*T*-$TiSe_2$. The transition is ascribed to inversion of Se 4*p* and Ti 3*d* bands with different parity at the Γ-point. It is very likely that the pressure range in which the topologically nontrivial phase emerges overlaps with the one of the superconductivity, leading to self-induced topological surface superconductivity in pressurized 1*T*-$TiSe_2$. As a consequence, the formation of topological superconducting surface states becomes accessible to an experimental investigation in the present material for appropriate electron doping. The surface state is promising for the realization of Majorana quasiparticle exitations because of the absence of lattice and chemical potential mismatches. We emphasize that the existence of the topological phase transition is guaranteed by spin-orbit coupling. For obtaining the pressure range of the self-induced topological surface superconductivity more exactly further experiments are required to determine the structure parameters under pressure with high accuracy. As s-type pairing is needed for topological superconducting surface states to occur, a more careful study is required to verify the conclusions of Ref. 35.

Methods

The high temperature normal structure of pristine 1*T*-$TiSe_2$ shows the space group $P\bar{3}m1$ (No. 164) where the Ti and Se atoms occupy 1*a* [(0, 0, 0)] and 2*d* [(1/3, 2/3, *z*)] sites, respectively, see Fig. 1(a). Experiments under ambient pressure yield structure parameters of $a = 3.54$ Å, $c = 6.008$ Å, and $z = 0.25504$[50]. Our full-potential linearized augmented plane wave calculations have been performed using the WIEN2k package[51]. We employ a threshold energy of −6.0 Ry for separating the valence and the core states, a muffintin radius of $R_{mt} = 2.2$ a_B, high values of $R_{mt}K_{max} = 10$ and $\ell_{max} = 10$, as well as a $20 \times 20 \times 10$ k-mesh. Moreover, a combination of the modified Becke-Johnson exchange potential and the local density approximation of the correlation potential is used in order to predict band gaps and band orders with an accuracy similar to hybrid functionals and Gutzwiller calculations[52]. Spin-orbit coupling is treated applying a second-variational method with a scalar relativistic basis. States up to 10 Ry above the Fermi energy (E_F) are included in the basis expansion.

1. Wilczek, F. Majorana returns. *Nature Phys.* **5**, 614–618 (2009).
2. Hasan, M. Z. & Kane, C. L. Colloquium: Topological insulators. *Rev. Mod. Phys.* **82**, 3045–3067 (2010).
3. Qi, X.-L. & Zhang, S.-C. Topological insulators and superconductors. *Rev. Mod. Phys.* **83**, 1057–1110 (2011).
4. Nayak, C. *et al.* Non-Abelian anyons and topological quantum computation. *Rev. Mod. Phys.* **80**, 1083–1159 (2008).
5. Read, N. & Green, D. Paired states of fermions in two dimensions with breaking of parity and time-reversal symmetries and the fractional quantum Hall effect. *Phys. Rev. B* **61**, 10267–10297 (2000).
6. Mackenzie, A. P. & Maeno, Y. The superconductivity of Sr_2RuO_4 and the physics of spin-triplet pairing. *Rev. Mod. Phys.* **75**, 657–712 (2003).
7. Das Sarma, S., Nayak, C. & Tewari, S. Proposal to stabilize and detect half-quantum vortices in strontium ruthenate thin films: Non-Abelian braiding statistics of vortices in a $p_x + ip_y$ superconductor. *Phys. Rev. B* **73**, 220502(R) (2006).
8. Björnsson, P. G., Maeno, Y., Huber, M. E. & Moler, K. A. Scanning magnetic imaging of Sr_2RuO_4. *Phys. Rev. B* **72**, 012504 (2005).
9. Kirtley, J. R. *et al.* Upper limit on spontaneous supercurrents in Sr_2RuO_4. *Phys. Rev. B* **76**, 014526 (2007).
10. Fu, L. & Kane, C. L. Superconducting proximity effect and Majorana fermions at the surface of a topological insulator. *Phys. Rev. Lett.* **100**, 096407 (2008).
11. Qi, X. L., Hughes, T. L. & Zhang, S.-C. Chiral topological superconductor from the quantum Hall state. *Phys. Rev. B* **82**, 184516 (2010).
12. Weng, H. *et al.* Half-metallic surface states and topological superconductivity in $NaCoO_2$ from first principles. *Phys. Rev. B* **84**, 060408(R) (2011).
13. Chung, S.-B., Zhang, H.-J., Qi, X.-L. & Zhang, S.-C. Topological superconducting phase and Majorana fermions in half-metal/superconductor heterostructures. *Phys. Rev. B* **84**, 060510(R) (2011).

14. Sau, J. D., Lutchyn, R. M., Tewari, S. & Das Sarma, S. Generic new platform for topological quantum computation using semiconductor heterostructures. *Phys. Rev. Lett.* **104**, 040502 (2010).
15. Alicea, J. *et al.* Non-Abelian statistics and topological quantum information processing in 1D wire networks. *Nature Phys.* **7**, 412–417 (2011).
16. Xia, Y. *et al.* Observation of a large-gap topological-insulator class with a single Dirac cone on the surface. *Nature Phys.* **5**, 398–402 (2009).
17. Zhang, H. *et al.* Topological insulators in Bi_2Se_3, Bi_2Te_3 and Sb_2Te_3 with a single Dirac cone on the surface. *Nature Phys.* **5**, 438–442 (2009).
18. Hsieh, D. *et al.* Observation of time-reversal-protected single-Dirac-cone topological-insulator states in Bi_2Te_3 and Sb_2Te_3. *Phys. Rev. Lett.* **103**, 146401 (2009).
19. Chen, Y. L. *et al.* Experimental realization of a three-dimensional topological insulator, Bi_2Te_3. *Science* **325**, 178–181 (2009).
20. Wray, L. A. *et al.* Observation of topological order in a superconducting doped topological insulator. *Nature Phys.* **6**, 855–859 (2010).
21. Hor, Y. S. *et al.* Superconductivity in $Cu_xBi_2Se_3$ and its implications for pairing in the undoped topological insulator. *Phys. Rev. Lett.* **104**, 057001 (2010).
22. Hosur, P., Ghaemi, P., Mong, R. S. K. & Vishwanath, A. Majorana modes at the ends of superconductor vortices in doped topological insulators. *Phys. Rev. Lett.* **107**, 097001 (2011).
23. Hor, Y. *et al.* Superconductivity and non-metallicity induced by doping the topological insulators Bi_2Se_3 and Bi_2Te_3. *J. Phys. Chem. Solids* **72**, 572–576 (2011).
24. Bay, T. V. *et al.* Superconductivity in the doped topological insulator $Cu_xBi_2Se_3$ under high pressure. *Phys. Rev. Lett.* **108**, 057001 (2012).
25. Einaga, M. *et al.* New superconducting phase of Bi_2Te_3 under pressure above 11 GPa. *J. Phys.: Conf. Ser.* **215**, 012036 (2010).
26. Di Salvo, F. J., Moncton, D. E. & Waszczak, J. V. Electronic properties and superlattice formation in the semimetal $TiSe_2$. *Phys. Rev. B* **14**, 4321–4328 (1976).
27. Morosan, E. *et al.* Superconductivity in Cu_xTiSe_2. *Nature Phys.* **2**, 544–550 (2006).
28. Qian, D. *et al.* Emergence of Fermi pockets in a new excitonic charge-density-wave melted superconductor. *Phys. Rev. Lett.* **98**, 117007 (2007).
29. Li, S. Y., Wu, G., Chen, X. H. & Taillefer, L. Single-gap s-wave superconductivity near the charge-density-wave quantum critical point in Cu_xTiSe_2. *Phys. Rev. Lett.* **99**, 107001 (2007).
30. Zhao, J. F. *et al.* Evolution of the electronic structure of 1T-Cu_xTiSe_2. *Phys. Rev. Lett.* **99**, 146401 (2007).
31. Bud'ko, S. L. *et al.* Thermal expansion and effect of pressure on superconductivity in Cu_xTiSe_2. *J. Phys.: Condens. Matter* **19**, 176230 (2007).
32. Barath, H. *et al.* Quantum and classical mode softening near the charge-density-wave-superconductor transition of Cu_xTiSe_2. *Phys. Rev. Lett.* **100**, 106402 (2008).
33. Jishi, R. A. & Alyahyaei, H. M. Electronic structure of superconducting copper intercalated transition metal dichalcogenides: First-principles calculations. *Phys. Rev. B* **78**, 144516 (2008).
34. Kusmartseva, A. F. *et al.* Pressure induced superconductivity in pristine 1T-$TiSe_2$. *Phys. Rev. Lett.* **103**, 236401 (2009).
35. Calandra, M. & Mauri, F. Charge-density wave and superconducting dome in $TiSe_2$ from electron-phonon interaction. *Phys. Rev. Lett.* **106**, 196406 (2011).
36. Yu, Y. G. & Ross, N. L. First-principles study on thermodynamic properties and phase transitions in TiS_2. *J. Phys.: Condens. Matter* **23**, 055401 (2011).
37. Allan, D. R. *et al.* High-pressure semiconductor-semimetal transition in TiS_2. *Phys. Rev. B* **57**, 5106–5110 (1998).
38. Fang, C. M., de Groot, R. A. & Haas, C. Bulk and surface electronic structure of 1T-TiS_2 and 1T-$TiSe_2$. *Phys. Rev. B* **56**, 4455–4463 (1997).
39. Fu, L. & Kane, C. L. Topological insulators with inversion symmetry. *Phys. Rev. B* **76**, 045302 (2007).
40. Zhu, Z. Y., Cheng, Y. C. & Schwingenschlögl, U. Topological phase transition in layered GaS and GaSe. *Phys. Rev. Lett.* **108**, 266805 (2012).
41. Aksoy, R., Selvi, E., Knudson, R. & Ma, Y. A high pressure x-ray diffraction study of titanium disulfide. *J. Phys.: Condens. Matter* **21**, 025403 (2009).
42. Kane, C. L. & Mele, E. J. Z_2 topological order and the quantum spin Hall effect. *Phys. Rev. Lett.* **95**, 146802 (2005).
43. Bernevig, B. A., Hughes, T. L. & Zhang, S.-C. Quantum spin Hall effect and topological phase transition in HgTe quantum wells. *Science* **314**, 1757–1761 (2006).
44. König, M. *et al.* Quantum spin Hall insulator state in HgTe quantum wells. *Science* **318**, 766–770 (2007).
45. Fu, L., Kane, C. L. & Mele, E. J. Topological insulators in three dimensions. *Phys. Rev. Lett.* **98**, 106803 (2007).
46. Moore, J. E. & Balents, L. Topological invariants of time-reversal-invariant band structures. *Phys. Rev. B* **75**, 121306(R) (2007).
47. Qi, X.-L., Hughes, T. L. & Zhang, S.-C. Topological field theory of time-reversal invariant insulatorsTopological field theory of time-reversal invariant insulators. *Phys. Rev. B* **78**, 195424 (2008).
48. Roy, R. Topological phases and the quantum spin Hall effect in three dimensions. *Phys. Rev. B* **79**, 195322 (2009).
49. Hsieh, D. *et al.* A topological Dirac insulator in a quantum spin Hall phase. *Nature* **452**, 970–974 (2008).
50. Riekel, C. Structure refinement of $TiSe_2$ by neutron diffraction. *J. Solid State Chem.* **17**, 389–392 (1976).
51. Blaha, P. *et al.* WIEN2k, An augmented plane wave plus local orbitals program for calculating crystal properties. *TU Vienna* (2001).
52. Tran, F. & Blaha, P. Accurate band gaps of semiconductors and insulators with a semilocal exchange-correlation potential. *Phys. Rev. Lett.* **102**, 226401 (2009).

Author contributions

Z.Z. and U.S. conceived the study and wrote the manuscript. Z.Z. and Y.C. performed the calculations.

Additional information

Competing financial interests: The authors declare no competing financial interests.

How to cite this article: Zhu, Z.Y., Cheng, Y.C. & Schwingenschlögl, U. Pressure controlled transition into a self-induced topological superconducting surface state. *Sci. Rep.* **4**, 4025; DOI:10.1038/srep04025 (2014).